

# Molecular dynamics simulation of cationic complexation with natural organic matter

A. G. KALINICHEV & R. J. KIRKPATRICK

Department of Geology and NSF WaterCAMPWS, University of Illinois at Urbana-Champaign, Urbana, IL 61801, USA

## Summary

Molecular computer modelling of natural organic matter (NOM) and its interactions with metal cations in aqueous solution is a highly effective tool for helping to understand and quantitatively predict the molecular mechanisms of metal-NOM complexation. This paper presents the results of molecular dynamics (MD) computations of the interaction of NOM with dissolved  $\text{Na}^+$ ,  $\text{Cs}^+$ ,  $\text{Mg}^{2+}$  and  $\text{Ca}^{2+}$ . They show that  $\text{Na}^+$  forms only very weak outer-sphere complexes with NOM, whereas  $\text{Cs}^+$  interacts somewhat more strongly, but also mainly via outer-sphere association.  $\text{Mg}^{2+}$  interacts little with NOM due to its strongly held hydration shell.  $\text{Ca}^{2+}$  has the strongest association with NOM and forms inner-sphere complexes with NOM carboxylate groups. This last result supports the idea of supramolecular, Ca-mediated NOM aggregation. Cation-NOM binding occurs principally with carboxylate groups, and to a lesser extent with phenolic and other  $-\text{R-OH}$  groups. The contributions of other NOM functional groups are minimal. The diffusional mobility of NOM-bound cations is  $\sim 20\%$  (NOM- $\text{Na}^+$  outer-sphere complex) to  $\sim 95\%$  (NOM- $\text{Ca}^{2+}$  inner-sphere complex) less than in aqueous solutions without NOM. The MD simulation results are in good agreement with NMR spectroscopic measurements for Cs-NOM solutions.

## Introduction

Natural organic matter (NOM) plays a variety of important roles in soil (Sposito, 1989; Stevenson, 1994), and its interaction with metal ions, minerals and organic species allows it to form water-soluble and water-insoluble complexes of widely differing chemical and biological stabilities. There are strong correlations between the concentration of natural organic matter and the speciation, solubility and toxicity of many trace metals, due to metal-NOM interaction (Buffle, 1988; Tipping, 2002). NOM is also one of the major causes of so-called ‘bio-fouling’ of nano-filtration and reverse osmosis membranes used industrially for water purification and desalination (e.g. Hong & Elimelech, 1997; Li & Elimelech, 2004; Lee & Elimelech, 2006).

However, the molecular-scale mechanisms and dynamics of the processes and reactions involving NOM are not well understood. NOM is compositionally and structurally heterogeneous, with reported apparent molecular weights ranging from a few hundred to several hundred thousand daltons. Whether NOM is chemically a true macromolecular entity or is merely a supramolecular assemblage of relatively small molecules held together by relatively weak non-covalent interactions is still under discussion

(Swift, 1999; Haynes & Clapp, 2001; Piccolo, 2002; Leenheer & Croué, 2003; Wershaw, 2004; Sutton & Sposito, 2005), but most recent experimental evidence seems to support the latter view (Simpson *et al.*, 2002; Peña-Méndez *et al.*, 2005). These compositional and structural uncertainties have limited generally applicable quantitative characterization of metal-NOM complexation in molecular-scale detail. Experimental results show that the extent of metal-NOM binding varies with the size, composition and configuration of the NOM, the pH and the ionic strength of the solution, the chemical properties of the metal, and the metal/NOM compositional ratio (Buffle, 1988; Tipping, 2002; Ritchie & Perdue, 2003). Combined experimental  $^{133}\text{Cs}$  and  $^{35}\text{Cl}$  NMR and computational molecular dynamics (MD) studies in our laboratory have provided a detailed, molecular-scale picture of the structural environments, dynamical behaviour, and mechanisms of chemical interaction among  $\text{Cs}^+$ ,  $\text{Cl}^-$  and Suwannee River NOM in aqueous solution (Xu *et al.*, 2006). Here we extend the molecular modelling approach to include several other important cations:  $\text{Na}^+$ ,  $\text{Mg}^{2+}$  and  $\text{Ca}^{2+}$ .

Computational molecular modelling is widely used in modern chemical, biological and materials sciences (e.g. Allen & Tildesley, 1987), and its application in geosciences has progressed rapidly in recent years (e.g. Cygan *et al.*, 2001). However, these

Correspondence: Andrey G. Kalinichev. E-mail: kalinich@uiuc.edu  
Received 7 September 2006; revised version accepted 8 May 2007

techniques have only rarely been applied to the investigation of NOM and its interaction with aqueous solutions and mineral surfaces (Schulten & Schnitzer, 1997; Leenheer *et al.*, 1998; Kubicki & Apitz, 1999; Sein *et al.*, 1999; Shevchenko *et al.*, 1999; Diallo *et al.*, 2003; Porquet *et al.*, 2003; Sutton *et al.*, 2005). Classical molecular computer simulations are typically performed for a relatively small system of  $100 < N < 100\,000$  particles (atoms, ions, and/or molecules) confined in a box with so-called 'periodic boundary conditions'. Using the rigorous formalism of statistical mechanics to analyse the large number of computer-generated instantaneous molecular configurations, these methods can yield many important thermodynamic, structural, spectroscopic, and transport properties of the simulated systems (e.g. Allen & Tildesley, 1987).

The greatest single challenge to effective molecular simulation is the ability to represent reliably the interactions between all atoms in the system. Computer simulations of NOM present significant additional challenges due to their extraordinary structural diversity and the fact that their structures and chemical compositions are not well defined. Thus, the level of detailed atomic-scale input often used for studies of crystalline materials is not readily available experimentally and is subject to considerable interpretation (e.g. Sein *et al.*, 1999; Diallo *et al.*, 2003; Leenheer & Croué, 2003).

There have been several efforts to develop molecular models of NOM. Schulten & Schnitzer (1997) used analytical pyrolysis measurements to develop a series of NOM structural models, and Sutton *et al.* (2005) used one such model in molecular simulations of NOM interaction with hydrated  $\text{Na}^+$  and  $\text{Ca}^{2+}$ . Shevchenko *et al.* (1999) simulated organo-mineral aggregates using an NOM model based on an oxidized lignin-carbohydrate complex. Diallo *et al.* (2003) developed a series of 3-D structural models for Chelsea soil humic acid by applying an algorithm of computer-assisted structure elucidation (CASE) to a comprehensive set of spectroscopic and analytical data for these substances. Leenheer *et al.* (1998) developed a model of Suwannee River fulvic acid and used it for the interpretation of experimental data on metal-NOM binding. Kubicki & Apitz (1999) used this model to compare relative structures computed by classical molecular mechanics and quantum (semi-empirical and Hartree-Fock) calculations and to test the effect of computational methodology on the predicted structure. This model was also used by Porquet *et al.* (2003) to study hydrogen bonding and clustering of neutral fulvic acid in aqueous solution. The Temple-Northeastern-Birmingham (TNB) model of an NOM building block was derived by Davies *et al.* (1997) from an earlier model of Steelink (1985) and was then successfully used in the conformational modelling study (Sein *et al.*, 1999).

The principal functional groups of NOM are well characterized (e.g. Stevenson, 1994; Leenheer & Croué, 2003), and the proposed NOM models have many common features. (The atomic composition of some of the models is compared with experimental data in Table 1). Thus, notwithstanding all the dif-

**Table 1** Composition of NOM building blocks according to several models

Model or data source	C	H	O	N	S	P	Carboxyl
	/wt%						/mol kg <sup>-1</sup> C
Steelink <sup>a</sup>	59.5	5.2	33.5	1.8	–	–	6.6
TNB <sup>b</sup>	57.4	4.9	34.0	3.7	–	–	7.0
CSHA#9 <sup>c</sup>	53.3	4.2	37.9	1.4	3.0	–	9.3
Schulten <sup>d</sup>	51.5	4.0	41.8	2.0	0.6	–	14.3
Exp. (SRNOM) <sup>e</sup>	52.5	4.2	42.7	1.1	0.6	0.02	9.85

<sup>a</sup>Steelink (1985).

<sup>b</sup>Davies *et al.* (1997).

<sup>c</sup>Diallo *et al.* (2003).

<sup>d</sup>Sutton *et al.* (2005).

<sup>e</sup>Experimental data for Suwannee River NOM (Ritchie & Perdue, 2003) are given for comparison.

ferences and uncertainties of the models, quantitative molecular-level modelling of metal-NOM binding in aqueous environment seems feasible and instructive.

## Methods

We have examined the use of the Steelink (1985) and TNB (Davies *et al.*, 1997) models of NOM monomers (Sein *et al.*, 1999) in MD simulations of cation complexation with NOM because of the similarity of their compositions to natural Suwannee River NOM used in the parallel  $\text{Cs}^+$  and  $\text{Cl}^-$  NMR studies (Xu *et al.*, 2006). Both models contain three carboxylic groups, three carbonyl groups, two phenolic groups, and four other R–OH alcohol groups. The TNB model also has two amine groups, whereas the Steelink model has only one. Both models have very similar structure and composition, and preliminary MD runs indicated negligible difference in their interactions with water and dissolved ions. Therefore, all of the production MD runs were performed with the TNB model, which corresponds somewhat more closely to the experimentally determined C/O/H composition of Suwannee River NOM. The molecular weight of the TNB model is 753 Da, which is within the range of the most frequently occurring NOM molecules of different origin as determined by multidimensional NMR spectroscopy (Simpson *et al.*, 2002) and mass spectrometry (Peña-Méndez *et al.*, 2005).

For the MD simulations, the model NOM molecule was hydrated by 556 water molecules in the cubic box with periodic boundary conditions (e.g. Allen & Tildesley, 1987). To simulate the situation of nearly neutral pHs, we assumed that all the NOM carboxylic groups are deprotonated and that the hydroxyl groups remain protonated. It is known experimentally that the carboxylic groups of NOM have  $pK_a$  values of 4–5 and are the principal source of their charge development, whereas the hydroxyl groups have  $pK_a$  values of  $\sim 9$  and contribute much less to negative charge development (Ritchie & Perdue, 2003).

The charge of the resulting NOM anion in our models was compensated by adding three mono-valent cations ( $\text{Na}^+$  or  $\text{Cs}^+$ ) or two di-valent cations ( $\text{Mg}^{2+}$  or  $\text{Ca}^{2+}$ ) and a  $\text{Cl}^-$ . All ions were originally placed in the bulk aqueous phase at least 7 Å from the NOM molecule and well separated from each other. In addition, we examined the concentration dependence of ionic complexation for the NOM-CsCl system from 0.3 to 4.0 M  $\text{Cs}^+$  (Xu *et al.*, 2006). Two representative snapshots of the Cs-NOM and Ca-NOM simulations illustrating the size and composition of the modelled systems are shown in Figure 1.

The interatomic interactions among  $\text{H}_2\text{O}$ , dissolved ions and NOM in our simulations are described by the simple point charge (SPC) water model of Berendsen *et al.* (1981), SPC-compatible parameters for the ions adapted from the literature (Åquist, 1990; Dang & Smith, 1993; Dang, 1995), and the consistent valency force field (CVFF) for the NOM (Kitson & Hagler, 1988). The CVFF model is also consistent with the SPC water model. The atomic charges and other parameters of the SPC water model are specifically optimized to reproduce not only the thermodynamic properties of bulk liquid water, such as density, vaporization energy, heat capacity, but also the structure of liquid water in terms of atom-atom radial distribution functions, which are experimentally known from X-ray and neutron diffraction measurements (Berendsen *et al.*, 1981). Over the past two decades, this water model has been thoroughly tested against various experimental data in numerous molecular simulations of aqueous systems, and despite its relative simplicity has proven to be one of the most reliable. (See, for example, Kalinichev (2001) and Jorgensen & Tirado-Rives (2005) for recent reviews).

For the simulations, Ewald summation was used to calculate long-range electrostatic contributions to the intermolecular potential energy, and 'spline cutoff' was applied to the short-range non-electrostatic interactions (e.g. Allen & Tildesley, 1987). A time step of 1.0 fs was used to integrate numerically the Newtonian equations of atomic motion in the MD algorithm. To assure proper thermodynamic equilibration and NOM conformational relaxation of the initially constructed molecular models, the pre-equilibration MD runs were performed for all simulated systems in several stages. First, a constant-volume (*NVT*-ensemble) MD simulation was run for 20 ps at a high temperature of 600 K. Then the temperature was decreased in steps of 50 K with the 20 ps *NVT*-ensemble MD simulation repeated at each temperature until the system was brought to the ambient temperature of 300 K. At this temperature an additional 20 ps pre-equilibration MD run was performed at a constant pressure of 100 kPa using the standard *NPT*-ensemble MD algorithm (e.g. Allen & Tildesley, 1987). This process resulted in simulated densities that correspond well to ambient pressure, and these optimized models were used as the starting configurations for the production MD simulations that were all performed in the *NVT*-ensemble at 300 K. Each system was allowed to equilibrate for the addi-

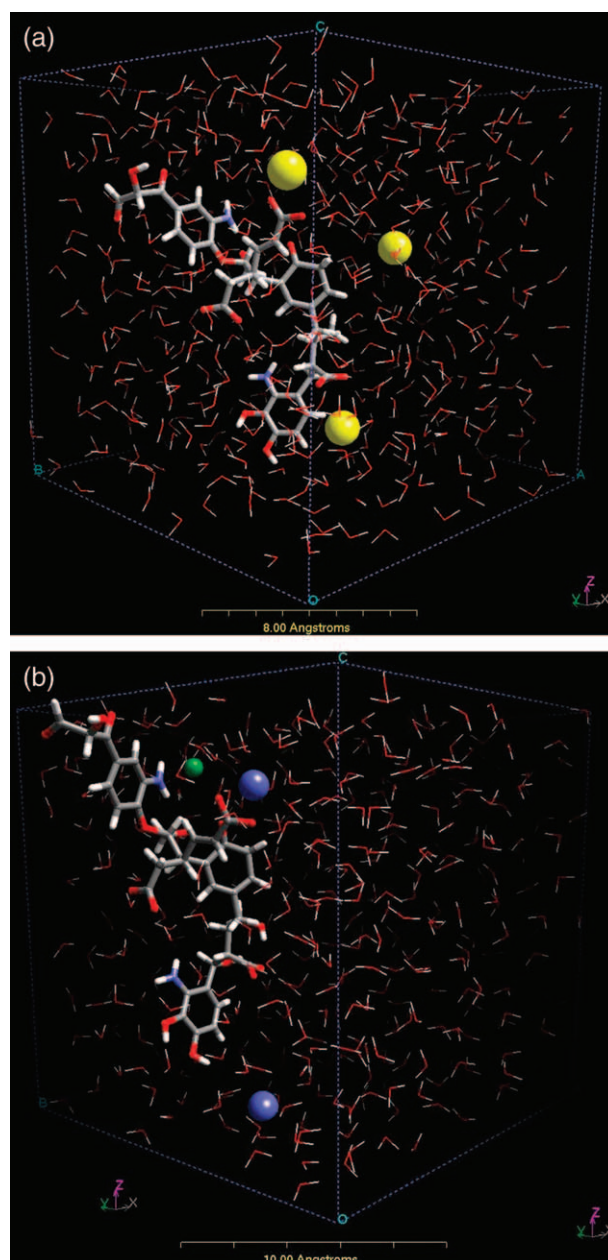


**Figure 1** Snapshots of NOM simulations of aqueous solutions with 0.3M  $\text{Cs}^+$  and 0.2 M  $\text{Ca}^{2+}$ . (a) Two  $\text{Cs}^+$  ions (yellow balls) are in outer-sphere coordination to the NOM molecule, and one remains in the bulk aqueous solution. (b) One  $\text{Ca}^{2+}$  ion (blue ball) is in inner-sphere coordination to the NOM molecule, and the other  $\text{Ca}^{2+}$  and the  $\text{Cl}^-$  ion (green ball) remain in the bulk aqueous solution.

tional 50 ps before the equilibrium dynamic trajectory for each model was finally recorded for statistical analysis at 10-fs intervals during a final 100 ps of MD simulation. Aqueous salt solutions with no NOM present were also simulated for reference purposes. In these MD runs, for each composition the volume of the MD simulation box was initially adjusted to

reproduce the experimentally known solution densities under ambient conditions.

To assess quantitatively the structural and dynamic effects of NOM-cation complexation, we calculated the radial distribution functions (RDFs), running coordination numbers, and diffusion coefficients of all aqueous species from the simulation results using standard procedures (e.g. Allen & Tildesley, 1987). The running coordination numbers of species  $j$  around species  $i$  in the solution,  $n_{ij}(r)$ , are calculated from the RDFs as

$$n_{ij}(r) = 4\pi\rho_j \int_0^{r_{i,\max}} g_{ij}(r) r^2 dr, \quad (1)$$

where  $\rho_j$  is the number density of species  $j$  in the system,  $g_{ij}(r)$  are the atom-atom RDFs, and  $r_{i,\max}$  is the cutoff radius characterizing the size of the coordination shell which was defined on the basis of the computed positions of the RDF minima for the corresponding ions.

The diffusion coefficients of all aqueous species were calculated from their mean square displacement using standard approaches (e.g. Allen & Tildesley, 1987):

$$D_i = \langle |\mathbf{r}_i(t) - \mathbf{r}_i(0)|^2 \rangle / 6N_i t, \quad (2)$$

where  $N_i$  is the number of species  $i$  in the simulated system,  $\mathbf{r}_i$  is the position of the atom,  $t$  is the time, and angular brackets denote the time-averaging along the dynamic trajectory of the simulated system and over all species  $i$  present in the solution.

## Results and discussion

The Na-NOM simulations (Figures 2a and 3a) show that  $\text{Na}^+$  ions interact only weakly with the model NOM as outer sphere complexes and remain almost entirely in the solution and fully hydrated by water molecules. The radii of the first and second coordination shells around  $\text{Na}^+$  are  $r_{\text{Na,max}}^{\text{I}} = 3.2 \text{ \AA}$  and  $r_{\text{Na,max}}^{\text{II}} = 5.6 \text{ \AA}$  (Figure 2a). This results in an average of  $\sim 6.0$   $\text{H}_2\text{O}$  molecules in the nearest neighbours (NN) coordination shell and  $\sim 26.0$  in the next-nearest neighbours (NNN) coordination to  $\text{Na}^+$  (out of scale in Figure 3a). No other species ever occur in the NN environment of  $\text{Na}^+$ , although there is detectable NNN coordination of  $\text{Na}^+$  by O-atoms of the NOM carboxylate groups (dashed line in Figure 3a), adding  $\sim 0.3$  to the NNN coordination. Thus,  $\text{Na}^+$  does not bind to any sites of NOM and even its outer-sphere coordination to the carboxylate groups is statistically marginal. This result agrees qualitatively very well with the recent molecular simulations of Sutton *et al.* (2005), but a direct quantitative comparison is not possible because of the different ways the simulations were performed. To create a more realistic model of NOM hydration and ionic complexation that allows for unrestricted ion exchange among inner-sphere, outer-sphere, and bulk-solution environments, we used peri-

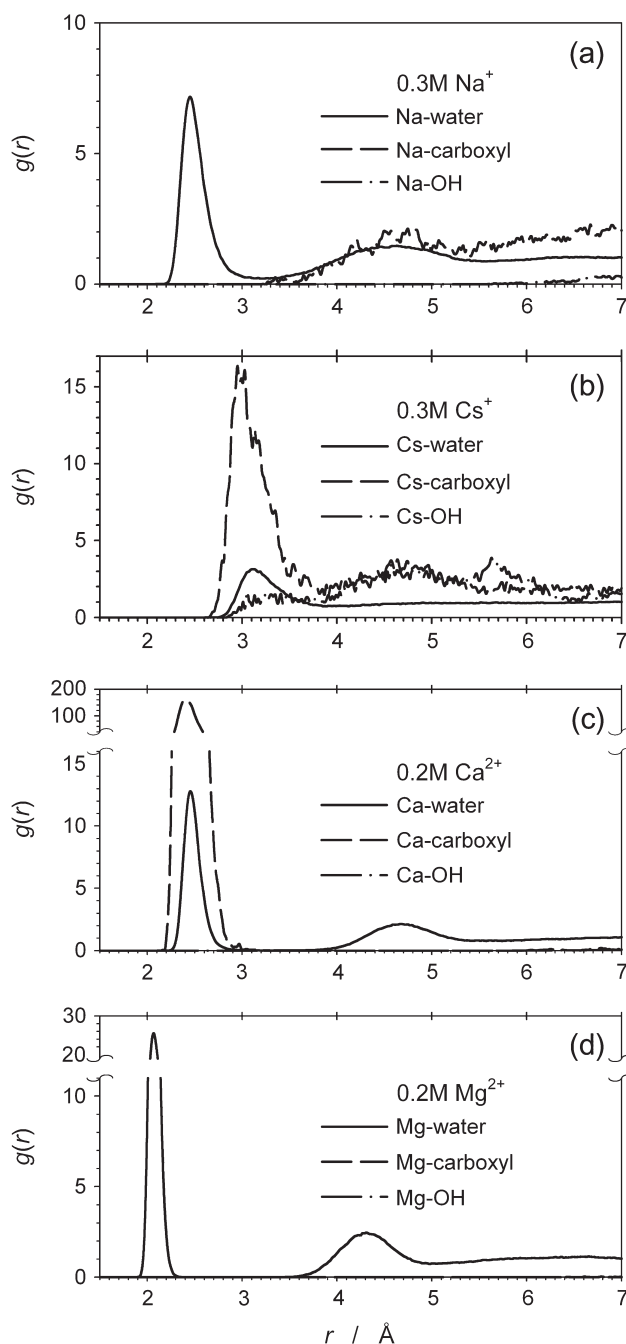


**Figure 2** MD-simulated radial distribution functions of  $\text{Na}^+$ ,  $\text{Cs}^+$ ,  $\text{Ca}^{2+}$ , and  $\text{Mg}^{2+}$  cation coordination with various species in aqueous NOM solution. Dashed and dash-dotted lines are, respectively, oxygen atoms of carboxyl and hydroxyl functional groups of the NOM molecule, and full lines are oxygen of  $\text{H}_2\text{O}$  in the solution.

odic boundary conditions with a large number of  $\text{H}_2\text{O}$  molecules. In contrast, Sutton *et al.* (2005) used a much larger NOM model, but without periodic boundary conditions. Their NOM molecule was hydrated by a thin, approximately  $5 \text{ \AA}$ , water layer, and all the  $\text{Na}^+$  ions were originally placed within

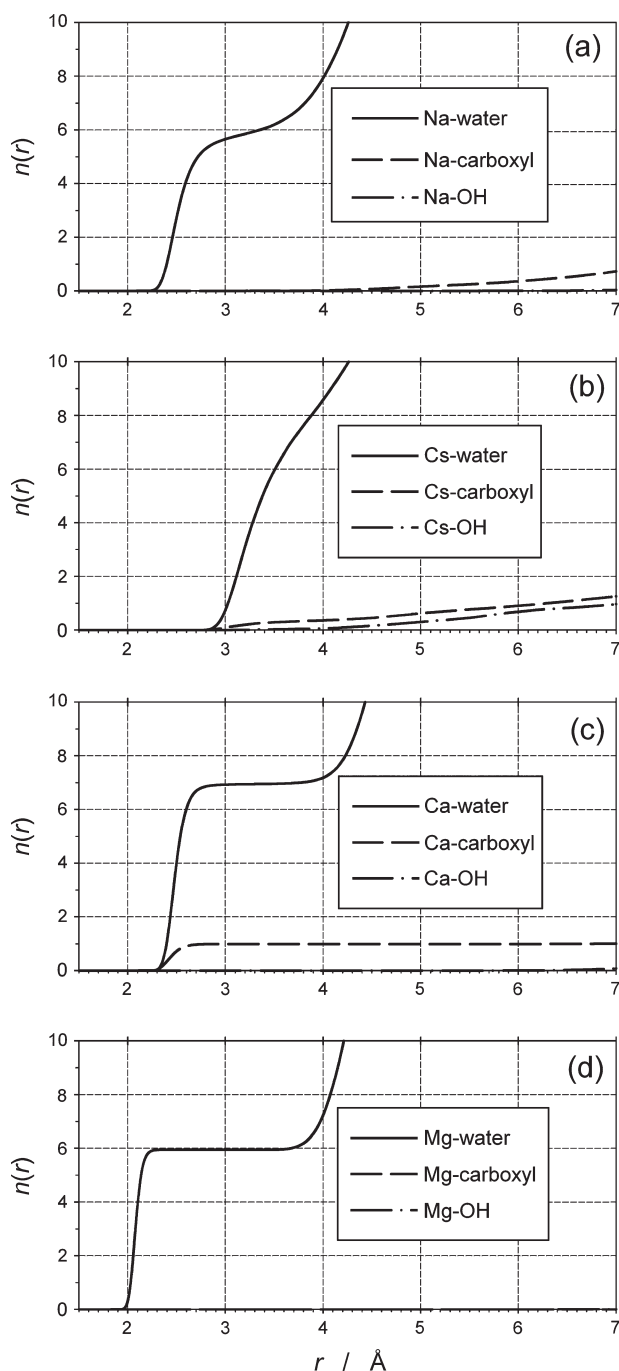


**Figure 3** MD-simulated running coordination numbers of  $\text{Na}^+$ ,  $\text{Cs}^+$ ,  $\text{Ca}^{2+}$ , and  $\text{Mg}^{2+}$  cation coordination with various species in aqueous NOM solution. Dashed and dash-dotted lines are, respectively, oxygen atoms of carboxyl and hydroxyl functional groups of the NOM molecule, and full lines are oxygen of  $\text{H}_2\text{O}$  in the solution.

$5.2 \text{ \AA}$  of the NOM carboxylate groups. Both of these circumstances lead to a bias in favour of the ions occurring in inner-sphere and outer-sphere coordination and the thin water shell precludes the possibility of the ions occurring in a fully

hydrated, bulk-solution environment. Nonetheless, the similarity of the results in our simulations and those of Sutton *et al.* is encouraging and suggests that the fundamental character of the ion–NOM interaction is not highly model-dependent.

For the Cs–NOM system, the simulated RDFs and running coordination numbers (Figures 2b and 3b) show a somewhat stronger  $\text{Cs}^+$  association with NOM. However, this association still occurs primarily via outer sphere complexes ( $r_{\text{Cs,max}}^{\text{I}} = 3.9 \text{ \AA}$  and  $r_{\text{Cs,max}}^{\text{II}} = 6.8 \text{ \AA}$ ). On average each  $\text{Cs}^+$  has  $\sim 8$  NN  $\text{H}_2\text{O}$  molecules,  $\sim 0.3$  NN O-atoms of the deprotonated NOM carboxylic groups, and  $\sim 0.1$  NN O-atoms of phenolic and other alcohol  $-\text{R}-\text{OH}$  groups of the NOM. None of the other NOM functional groups contribute to  $\text{Cs}^+$  binding. In the second coordination shell of  $\text{Cs}^+$  there are  $\sim 40$   $\text{H}_2\text{O}$  molecules,  $\sim 1$  O-atom of the NOM carboxylate groups, and  $\sim 1$  O-atom of the phenolic and other alcohol groups. With increasing CsCl solution concentration, the Cs–NOM association decreases gradually and is replaced by the stronger  $\text{Cs}^+ - \text{Cl}^-$  coordination in the solution (Xu *et al.*, 2006). At CsCl concentrations above  $0.4\text{--}0.5 \text{ M}$ , most of the  $\text{Cs}^+$  is not associated with the NOM, and the average  $\text{Cs}^+$  NN and NNN coordination shells are nearly identical to those of CsCl solutions without NOM present.

$\text{Ca}^{2+}$  ions interact with NOM more strongly than any other species studied here, and can occur in well-defined inner-sphere complexes (Figures 2c and 3c). During the pre-equilibration stage of the simulations, one out of the two  $\text{Ca}^{2+}$  ions was adsorbed by one of the NOM carboxylate groups and remained in this environment for the entire duration of the equilibrium MD run. For this  $\text{Ca}^{2+}$  one carboxylate group replaced two (out of eight) water molecules in the first coordination shell. In contrast, the other  $\text{Ca}^{2+}$  remained in the bulk aqueous solution and did not associate with the NOM molecule even by outer-sphere complexation. Thus, averaging over the entire simulated system (Figure 3c),  $\sim 1.0$  O atom of carboxylate groups occurs in the first and second coordination shells of  $\text{Ca}^{2+}$  ( $r_{\text{Ca,max}}^{\text{I}} = 3.2 \text{ \AA}$ ;  $r_{\text{Ca,max}}^{\text{II}} = 5.6 \text{ \AA}$ ). No other functional groups contribute to the  $\text{Ca}^{2+}$ –NOM complexation. These results are also in good agreement with the simulations of Sutton *et al.* (2005), who observed  $\sim 1.29$  NOM carboxylate O atoms in the first coordination shell of  $\text{Ca}^{2+}$ . As for the  $\text{Na}^+$ –NOM complexation discussed above, some quantitative discrepancies between the two sets of simulations should be expected, because of the differences in how they were performed.

Our results for the Mg–NOM system reveal no association of  $\text{Mg}^{2+}$  ions with NOM whatsoever (Figures 2d and 3d). Whether NOM is present in solution or not, each  $\text{Mg}^{2+}$  ion is hydrated by  $\sim 6.0$   $\text{H}_2\text{O}$  molecules in the first coordination shell, and  $\sim 22.3$   $\text{H}_2\text{O}$  molecules in the second coordination shell ( $r_{\text{Mg,max}}^{\text{I}} = 2.5 \text{ \AA}$ ;  $r_{\text{Mg,max}}^{\text{II}} = 5.2 \text{ \AA}$ ). The particularly strong, well-defined second hydration shell probably explains why  $\text{Mg}^{2+}$  ions do not associate significantly with the negatively charged functional groups of NOM.

Overall, the relative strength of the metal-NOM complexation, as shown by the present MD simulations and those of Sutton *et al.* (2005), are best interpreted in terms of simple electrostatic considerations as described by the charge/radius ( $z/R$ ) ratio of the cation. For instance,  $\text{Ca}^{2+}$  is nearly the same size as  $\text{Na}^+$  ( $R_{\text{Ca}} = 1.61 \text{ \AA}$ ,  $R_{\text{Na}} = 1.45 \text{ \AA}$ ) but interacts more strongly with the NOM carboxylate groups due to its larger  $z/R$  (1.24 vs. 0.69  $e/\text{\AA}$ ). In contrast, for ions with the same charge ( $\text{Na}^+$  vs.  $\text{Cs}^+$ , or  $\text{Mg}^{2+}$  vs.  $\text{Ca}^{2+}$ ), the larger ions show stronger association with NOM because water molecules in their hydration shells are less strongly held ( $R_{\text{Cs}} = 2.15 \text{ \AA}$ ,  $R_{\text{Mg}} = 0.92 \text{ \AA}$ ).

These results also suggest that  $\text{Ca}^{2+}$  complexation with the negatively charged functional groups of NOM and the surfaces of nanofiltration membranes used in water purification play a key role in fouling of the membranes by NOM (e.g. Li & Elimelech, 2004). Such membranes typically contain large concentrations of carboxylate groups. The experimental results show that such fouling occurs with water that contains  $\text{Ca}^{2+}$  but not  $\text{Mg}^{2+}$  (Li & Elimelech, 2004; Lee & Elimelech, 2006). Thus, it appears that successful competition for coordination to the cations by negatively charged O atoms of the membrane and NOM functional groups allows  $\text{Ca}^{2+}$  to bridge the NOM and membrane polymer via Coulombic interactions alone and that the strong preference of  $\text{Mg}^{2+}$  for  $\text{H}_2\text{O}$  prevents this interaction. These results also suggest that similar electrostatic linkages of relatively small NOM fragments by  $\text{Ca}^{2+}$  ions, rather than much weaker dispersive and hydrogen bonding interactions, can provide the predominant mechanism of the formation of large supramolecular NOM aggregates (e.g. Piccolo, 2002; Wershaw, 2004).

The computed diffusion properties of the ions in NOM solutions are consistent with these structural interpretations. In Table 2 they are also compared with available simulation results for similar aqueous salt solutions without NOM (Obst & Bradaczek, 1996; Lee & Rasaiah, 1996). Due to the relatively small number of ions in our simulated systems, the statistical uncertainties of calculated diffusion coefficients are relatively large (Figure 4, Table 2). Applying Equation (2) separately to several shorter fragments of each simulated MD trajectory, we estimated the error bars to be on the order of 15–20%. However, within this level of uncertainty, some quantitative comparisons are well justified. For the alkali cations,  $D_{\text{Na}}$  is only slightly reduced by the presence of NOM due to the weak outer sphere  $\text{Na}^+$ –NOM complexation.  $D_{\text{Cs}}$  is  $\sim 30\%$  smaller in the NOM–CsCl solution due to its stronger association with the NOM molecule. We have recently shown that this effect rapidly diminishes with increasing CsCl concentration, due to decreased  $\text{Cs}^+$ –NOM interaction caused by increased  $\text{Cs}^+$ – $\text{Cl}^-$  ion pairing (Figure 5; Xu *et al.*, 2006). The computed low-frequency power spectra of  $\text{Cs}^+$  translational vibrations also show some effect of the presence of NOM on the  $\text{Cs}^+$  dynamics at the lowest CsCl concentration (Xu *et al.*, 2006).

For the alkaline earth cations, the mobility of  $\text{Ca}^{2+}$  is reduced much more by NOM than that of  $\text{Mg}^{2+}$ , reflecting the inner-

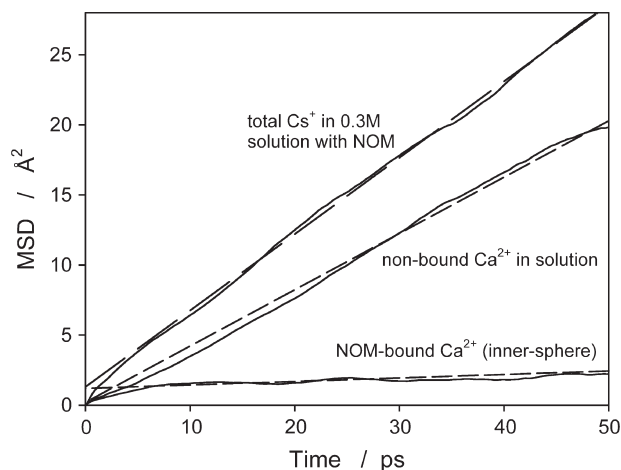


**Figure 4** Time dependence of  $\text{Cs}^+$  and  $\text{Ca}^{2+}$  mean square displacement in various environments (solid lines) and linear fits to these curves (dashed lines) illustrating the statistical accuracy of the estimated ionic diffusion coefficients.

sphere complexation of  $\text{Ca}^{2+}$  with NOM. Their diffusion coefficients differ by a factor of  $\sim 20$ , with the adsorbed  $\text{Ca}^{2+}$  closely following the diffusion of the NOM molecule (Table 2). In contrast,  $\text{Mg}^{2+}$  mobility is unaffected by the presence of NOM in the solution, in good agreement with the structural results discussed above.

For the Cs–NOM system, the results of the present MD simulations are also strongly supported by the structural and dynamical interpretations of the experimental  $^{133}\text{Cs}$  and  $^{35}\text{Cl}$  NMR data (Xu *et al.*, 2006). The essentially outer sphere association of  $\text{Cs}^+$  with the NOM is consistent with the experimental observation that NOM does not affect the  $^{133}\text{Cs}$  NMR chemical shift, since the computed average NN structure around

**Table 2** Diffusion coefficients of aqueous species in NOM solutions

Aqueous species	$D_i$ / $10^{-5} \text{ cm}^2 \text{ s}^{-1}$	
	$D_i$	$D_i^{\text{bulk}}$
$\text{Na}^+$	$1.0 \pm 0.2$	$\begin{cases} 1.21 \pm 0.2 \\ 1.22 \pm 0.05^{\text{a}} \\ 1.22 \pm 0.47^{\text{b}} \end{cases}$
$\text{Cs}^+$	$0.9 \pm 0.15$	$\begin{cases} 1.3 \pm 0.2 \text{ (at } 3 \text{ M CsCl)} \\ 1.8 \pm 0.2 \\ 2.0 \pm 0.3^{\text{b}} \end{cases}$ (at inf. dilution)
$\text{Ca}^{2+}$ (average)	$0.4 \pm 0.08$	–
$\text{Ca}^{2+}$ (inner-sphere)	$0.03 \pm 0.01$	–
$\text{Ca}^{2+}$ (bulk in NOM soln)	$0.7 \pm 0.15$	$0.55 \pm 0.04^{\text{a}}$
$\text{Mg}^{2+}$	$0.6 \pm 0.15$	$0.62 \pm 0.09^{\text{a}}$
NOM centre of mass	$0.05 \pm 0.03$	–

<sup>a</sup>Obst & Bradaczek (1996).

<sup>b</sup>Lee & Rasaiah (1996).

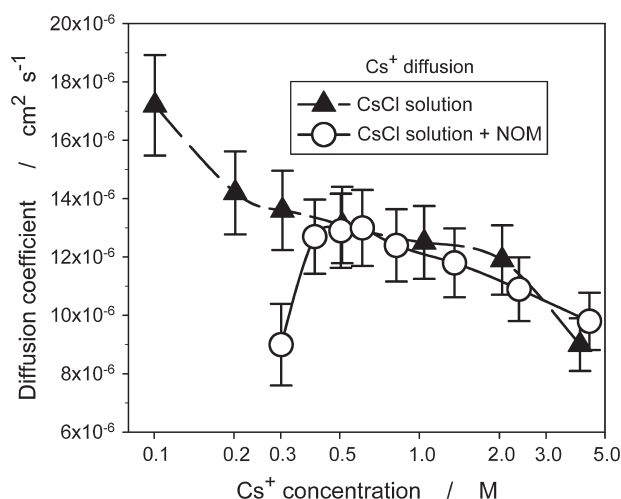


**Figure 5** MD-simulated diffusion coefficients of Cs<sup>+</sup> in CsCl-NOM aqueous solutions as a function of Cs<sup>+</sup> concentration. (Note the logarithmic concentration scale).

Cs<sup>+</sup> is not greatly affected by this association. The more preferential occurrence of Cs<sup>+</sup> near the NOM at low concentrations and the decreasing average Cs-NOM association with increasing CsCl concentration are also consistent with the experimentally observed increased <sup>133</sup>Cs 1/T<sub>1</sub> relaxation rate at low CsCl concentrations and the rapid convergence of this rate to a value typical of aqueous solutions without NOM at larger CsCl concentrations. Dynamically, the modest reduction in the Cs<sup>+</sup> diffusion coefficient due to NOM association is consistent with the narrow, solution-like <sup>133</sup>Cs resonances observed in the NMR spectra (Xu *et al.*, 2006).

## Conclusions

MD simulations of metal-NOM systems presented here and the results of other similar molecular modelling efforts (Sutton *et al.*, 2005; Xu *et al.*, 2006) clearly indicate that both the structural and dynamic aspects of the cation-NOM complexation follow a simple trend in terms of the charge/size ratio for the ions. Due to the competition between ion hydration in bulk aqueous solution and adsorption of these cations by the negatively charged NOM functional groups (primarily carboxylate), larger ions of the same charge (Cs<sup>+</sup> vs. Na<sup>+</sup>, or Ca<sup>2+</sup> vs. Mg<sup>2+</sup>) have a stronger tendency for NOM association. However, for ions of approximately the same size, higher charge results in a stronger association with NOM. Thus, in contrast to Mg<sup>2+</sup>, Ca<sup>2+</sup> forms strong inner-sphere complexes with NOM carboxylate groups, whereas the association of Na<sup>+</sup> with NOM is even weaker than the outer-sphere metal-NOM complexing observed for Cs<sup>+</sup>.

The case of Cs<sup>+</sup> complexation is particularly interesting. Cs<sup>+</sup> readily occurs as inner-sphere complexes on the surfaces of sil-

ica gel and many common soil minerals, including illite, kaolinite and boehmite (Kim *et al.*, 1996a,b). The weaker interaction with NOM may be due to the occurrence of relatively isolated carboxylic and phenolic groups on the NOM compared to densely packed structural oxygens and hydroxyl groups on the mineral surfaces. The trends of Cs-NOM association observed in our study are also quite similar to the sorption of NOMs with widely varying composition and structure onto goethite at approximately pH 4, as recently studied by Kaiser (2003) in batch sorption experiments. These results indicate interaction of negatively charged NOM with positively charged goethite surfaces, comparable to the interaction of NOM with dissolved Cs<sup>+</sup> in our simulations and NMR measurements (Xu *et al.*, 2006). The sorption of NOM onto goethite surfaces in all cases follows a Langmuir type isotherm, and the total number of NOM acidic groups positively and linearly controls the interaction between NOM and goethite.

Although the models of metal-NOM solutions studied in our present work are quite realistic and representative, they are still relatively small and statistically can capture only the interactions of individual ions with individual NOM functional groups. The current results can be interpreted as ~8% of NOM carboxylate groups being coordinated by Cs<sup>+</sup> or, alternatively, as up to ~17% Cs<sup>+</sup> in solution forming inner- and outer-sphere complexes with NOM. Similarly, we can conclude that ~50% of available Ca<sup>2+</sup> ions in solution form strong inner-sphere complexes with NOM carboxylate groups, or that ~33% of such groups are strongly complexed by Ca<sup>2+</sup>. Much larger systems with several independent (and, probably, structurally diverse) NOM fragments in aqueous salt solutions need to be simulated in order to probe quantitatively such important phenomena as cooperativity in metal-NOM complexation, the development of supramolecular metal-NOM aggregates and their conformational structure, and the formation of compact fouling layers on the surfaces of nanofiltration membranes (e.g. Li & Elimelech, 2004). These problems will be the focus of our future simulation efforts.

## Acknowledgements

This research was supported by DOE Basic Energy Sciences (Grant DEFGO2-00ER-15028) and the NSF Science and Technology Center of Advanced Materials for Purification of Water with Systems (WaterCAMPWS) at the University of Illinois. Computation was partially supported by the National Computational Science Alliance (Grant EAR 990003 N) and utilized Cerius2-4.9 software package from Accelrys. We thank Xiang Xu for useful discussions.

## References

Allen, M.P. & Tildesley, D.J. 1987. *Computer Simulation of Liquids*. Clarendon Press, Oxford.

- Åqvist, J. 1990. Ion–water interaction potentials derived from free-energy perturbation simulations. *Journal of Physical Chemistry*, **94**, 8021–8024.
- Berendsen, H.J.C., Postma, J.P.M., van Gunsteren, W.F. & Hermans, J. 1981. Interaction models for water in relation to protein hydration. In: *Intermolecular Forces* (ed. B. Pullman), pp. 331–342. Riedel, Dordrecht, The Netherlands.
- Buffle, J. 1988. *Complexation Reactions in Aquatic Systems: an Analytical Approach*. Ellis Horwood Ltd, Chichester.
- Cygan, R.T. & Kubicki, J.D. (eds) 2001. *Molecular Modeling Theory and Applications in the Geosciences. Reviews in Mineralogy and Geochemistry*, v.42. Mineralogical Society of America, Washington, DC.
- Dang, L.X. 1995. Mechanism and thermodynamics of ion selectivity in aqueous solutions of 18-crown-6 ether – a molecular dynamics study. *Journal of the American Chemical Society*, **117**, 6954–6960.
- Dang, L.X. & Smith, D.E. 1993. Molecular dynamics simulations of aqueous ionic clusters using polarizable water. *Journal of Chemical Physics*, **99**, 6950–6956.
- Davies, G., Fataftah, A., Cherkasskiy, A., Ghabbour, E.A., Radwan, A., Jansen, S.A. *et al.* 1997. Tight metal binding by humic acids and its role in biomineralization. *Journal of the Chemical Society – Dalton Transactions*, **21**, 4047–4060.
- Diallo, M.S., Simpson, A., Gassman, P., Faulon, J.-L., Johnson, J.H., Goddard, W.A. & Hatcher, P.G. 2003. 3-D structural modeling of humic acids through experimental characterization, computer-assisted structure elucidation and atomistic simulations. 1. Chelsea soil humic acid. *Environmental Science and Technology*, **37**, 1783–1793.
- Haynes, M.H.B. & Clapp, C.E. 2001. Humic substances: considerations of compositions, aspects of structure, and environmental influences. *Soil Science*, **166**, 723–737.
- Hong, S.K. & Elimelech, M. 1997. Chemical and physical aspects of natural organic matter (NOM) fouling of nanofiltration membranes. *Journal of Membrane Science*, **132**, 159–181.
- Jorgensen, W.L. & Tirado-Rives, J. 2005. Potential energy functions for atomic-level simulations of water and organic and biomolecular systems. *Proceedings of the National Academy of Sciences of the USA*, **102**, 6665–6670.
- Kaiser, K. 2003. Sorption of natural organic matter fractions to goethite (alpha-FeOOH): effect of chemical composition as revealed by liquid-state <sup>13</sup>C NMR and wet-chemical analysis. *Organic Geochemistry*, **34**, 1569–1579.
- Kalinichev, A.G. 2001. Molecular simulations of liquid and supercritical water: thermodynamics, structure, and hydrogen bonding. *Reviews in Mineralogy and Geochemistry*, **42**, 83–129.
- Kim, Y., Cygan, R.T. & Kirkpatrick, R.J. 1996a. <sup>133</sup>Cs NMR and XPS investigation of cesium adsorbed on clay minerals and related phases. *Geochimica et Cosmochimica Acta*, **60**, 1041–1052.
- Kim, Y., Kirkpatrick, R.J. & Cygan, R.T. 1996b. <sup>133</sup>Cs NMR study of cesium on the surfaces of kaolinite and illite. *Geochimica et Cosmochimica Acta*, **60**, 4059–4074.
- Kitson, D.H. & Hagler, A.T. 1988. Theoretical studies of the structure and molecular dynamics of a peptide crystal. *Biochemistry*, **27**, 5246–5257.
- Kubicki, J.D. & Apitz, S.E. 1999. Models of natural organic matter and interactions with organic contaminants. *Organic Geochemistry*, **30**, 911–927.
- Lee, S. & Elimelech, M. 2006. Relating organic fouling of reverse osmosis membranes to intermolecular adhesion forces. *Environmental Science and Technology*, **40**, 980–987.
- Lee, S.H. & Rasaiah, J.C. 1996. Molecular dynamics simulation of ion mobility. 2. Alkali metal and halide ions using the SPC/E model for water at 25°C. *Journal of Physical Chemistry*, **100**, 1420–1425.
- Leenheer, J.A., Brown, G.K., MacCarthy, P. & Cabaniss, S.E. 1998. Models of metal binding structures in fulvic acid from the Suwannee River, Georgia. *Environmental Science and Technology*, **32**, 2410–2416.
- Leenheer, J.A. & Croué, J.P. 2003. Characterizing aquatic dissolved organic matter. *Environmental Science and Technology*, **37**, 18A–26A.
- Li, Q.L. & Elimelech, M. 2004. Organic fouling and chemical cleaning of nanofiltration membranes: measurements and mechanisms. *Environmental Science and Technology*, **38**, 4683–4693.
- Obst, S. & Bradaczek, H. 1996. Molecular dynamics study of the structure and dynamics of the hydration shell of alkaline and alkaline-earth metal cations. *Journal of Physical Chemistry*, **100**, 15677–15687.
- Peña-Méndez, E.M., Gajdošová, D., Novotná, K., Prošek, P. & Havel, J. 2005. Mass spectrometry of humic substances of different origin including those from Antarctica – a comparative study. *Talanta*, **67**, 880–890.
- Piccolo, A. 2002. The supramolecular structure of humic substances: a novel understanding of humus chemistry and implications in soil science. *Advances in Agronomy*, **75**, 57–134.
- Porquet, A., Bianchi, L. & Stoll, S. 2003. Molecular dynamic simulations of fulvic acid clusters in water. *Colloids and Surfaces A – Physicochemical and Engineering Aspects*, **217**, 49–54.
- Ritchie, J.D. & Perdue, E.M. 2003. Proton-binding study of standard and reference fulvic acids, humic acids, and natural organic matter. *Geochimica et Cosmochimica Acta*, **67**, 85–96.
- Schulten, H.R. & Schnitzer, M. 1997. Chemical model structures for soil organic matter and soils. *Soil Science*, **162**, 115–130.
- Sein, L.T., Varnum, J.M. & Jansen, S.A. 1999. Conformational modeling of a new building block of humic acid: approaches to the lowest energy conformer. *Environmental Science and Technology*, **33**, 546–552.
- Shevchenko, S.M., Bailey, G.W. & Akim, L.G. 1999. The conformational dynamics of humic polyanions in model organic and organo-mineral aggregates. *Journal of Molecular Structure (Theochem)*, **460**, 179–190.
- Simpson, A.J., Kingery, W.L., Hayes, M.H.B., Spraul, M., Humpfer, E., Dvortsak, P. *et al.* 2002. Molecular structures and associations of humic substances in the terrestrial environment. *Naturwissenschaften*, **89**, 84–88.
- Sposito, G. 1989. *The Chemistry of Soils*. Oxford University Press, New York.
- Steelink, C. 1985. Implications of elemental characteristics of humic substances. In: *Humic Substances in Soil, Sediment, and Water* (eds G.R. Aiken, D.M. McKnight & R.L. Wershaw), pp. 457–476. John Wiley, New York.
- Stevenson, F.J. 1994. *Humus Chemistry: Genesis, Composition, Reactions*, 2nd edn. John Wiley, New York.
- Sutton, R. & Sposito, G. 2005. Molecular structure in soil humic substances: the new view. *Environmental Science and Technology*, **39**, 9009–9015.
- Sutton, R., Sposito, G., Diallo, M.S. & Schulten, H.R. 2005. Molecular simulation of a model of dissolved organic matter. *Environmental Toxicology and Chemistry*, **24**, 1902–1911.

- Swift, R.S. 1999. Macromolecular properties of soil humic substances: fact, fiction, and opinion. *Soil Science*, **164**, 790–802.
- Tipping, E. 2002. *Cation Binding by Humic Substances*. Cambridge University Press, Cambridge.
- Wershaw, R.L. 2004. *Evaluation of Conceptual Models of Natural Organic Matter (Humus) from a Consideration of the Chemical and Biochemical Processes of Humification*. US Geological Survey Scientific Investigations Report 2004–5121. US Geological Survey, Reston, Virginia.
- Xu, X., Kalinichev, A.G. & Kirkpatrick, R.J. 2006.  $^{133}\text{Cs}$  and  $^{35}\text{Cl}$  NMR spectroscopy and molecular dynamics modeling of  $\text{Cs}^+$  and  $\text{Cl}^-$  complexation with natural organic matter. *Geochimica et Cosmochimica Acta*, **70**, 4319–4331.